



HAL
open science

Size and shape of ULF waves in the terrestrial foreshock

M. Archer, T.S. Horbury, E.A. Lucek, C. Mazelle, A. Balogh, J. Dandouras

► **To cite this version:**

M. Archer, T.S. Horbury, E.A. Lucek, C. Mazelle, A. Balogh, et al.. Size and shape of ULF waves in the terrestrial foreshock. *Geophysical Research Letters*, 2005, 110, pp.A05208. 10.1029/2004ja010791 . hal-00013047

HAL Id: hal-00013047

<https://hal.science/hal-00013047>

Submitted on 12 Feb 2021

HAL is a multi-disciplinary open access archive for the deposit and dissemination of scientific research documents, whether they are published or not. The documents may come from teaching and research institutions in France or abroad, or from public or private research centers.

L'archive ouverte pluridisciplinaire **HAL**, est destinée au dépôt et à la diffusion de documents scientifiques de niveau recherche, publiés ou non, émanant des établissements d'enseignement et de recherche français ou étrangers, des laboratoires publics ou privés.

Size and shape of ULF waves in the terrestrial foreshock

M. Archer,¹ T. S. Horbury,¹ E. A. Lucek,¹ C. Mazelle,² A. Balogh,¹ and I. Dandouras²

Received 16 September 2004; revised 7 March 2005; accepted 22 March 2005; published 20 May 2005.

[1] Using simultaneous four spacecraft data, estimates of the size and shape of ULF waves in the terrestrial foreshock are presented. Estimates of the size of the waves in different directions are obtained by calculating the spatial autocorrelation function of the magnetic field in the wave frame using cross-correlations of magnetic field measurements between the four Cluster spacecraft. The correlation length along the wave vector, its wavelength, is typically $1-3 R_E$, consistent with previous estimates. The correlation length perpendicular to the wave vector, however, is typically 3–8 times the wavelength, between 8 and $18 R_E$. The shape of the waves can be approximated as an oblate spheroid, symmetric around the wave vector. However, the wave front tends to be significantly more planar than a spheroid, implying planarity of the waves over several R_E and hence a coherent periodic variation of the magnetic field at the bow shock on these scales. There is some evidence that at least during one extended interval of ULF waves, their finite perpendicular extent results in an additional quasi-periodic enhancement and modulation of the waves, with a period of several minutes, at the spacecraft.

Citation: Archer, M., T. S. Horbury, E. A. Lucek, C. Mazelle, A. Balogh, and I. Dandouras (2005), Size and shape of ULF waves in the terrestrial foreshock, *J. Geophys. Res.*, *110*, A05208, doi:10.1029/2004JA010791.

1. Introduction

[2] Large-amplitude, quasi-periodic, ~ 30 s period waves (“ULF waves”) are frequently observed by spacecraft in the solar wind upstream of the Earth’s bow shock [e.g., *Hoppe and Russell*, 1983]. These waves are generated by instabilities between the solar wind plasma and ions backstreaming from the bow shock [*Gary*, 1985]. ULF waves are of interest not only as an example of a fundamental wave-particle interaction in collisionless plasmas: being of large amplitude ($|\delta\mathbf{B}|/B_0 \approx 1$), they also cause large changes in the magnetic field direction at the bow shock surface, and hence the magnetic field shock-normal angle, θ_{Bn} , resulting in periodic changes in bow shock properties [*Greenstadt and Mellott*, 1985]. Many basic properties of ULF waves are now well known (see, e.g., the review by *Burgess* [1997]): they are typically a few R_E in size along their wave vector and propagate $\sim 20-40^\circ$ from the local magnetic field. They propagate sunwards at speeds close to the local Alfvén speed in the plasma frame [*Mazelle et al.*, 2003] but are convected earthward into the shock by the faster solar wind flow. This convection also reverses their sense of polarization, which is usually right-handed in the plasma frame so that they appear left-handed in the spacecraft frame (relative to the magnetic field). The waves are often nearly sinusoidal but can also have steepened edges, sometimes with attendant whistler waves. These variations appear to be associated with changes in the

distribution of backstreaming ions [*Meziane et al.*, 2001; *Mazelle et al.*, 2003; *Meziane et al.*, 2004a].

[3] Recent data from the four spacecraft Cluster mission has made it possible to determine some properties of ULF waves more accurately than with a single spacecraft. *Eastwood et al.* [2002, 2003] estimated the wave vectors and modes of several intervals of ULF waves, finding broad agreement with previous estimates [*Hoppe and Russell*, 1983]. *Mazelle et al.* [2003] studied the distributions of ions within an interval of ULF waves. They argued that the ions were gyrophase bunched and pitch angle trapped by the waves, emphasising the importance of ULF waves in modulating upstream ions.

[4] The finite size and curvature of the Earth’s bow shock implies that any ULF wave field must be limited in extent. *Le and Russell* [1990] and *Le et al.* [1993] used cross-correlations of the magnetic field measured at the ISEE 1 and 2 spacecraft to estimate the spatial extent of foreshock ULF waves. They showed that the correlation between the spacecraft dropped to around 0.5 when their flow-perpendicular separation was around $1 R_E$, indicating that the waves were indeed finite in extent across the flow. More recently, *Eiges et al.* [2001] performed a similar analysis using mass flux measurements and obtained scales of around $2 R_E$. However, the limitations of using only two spacecraft meant that all of these studies used many intervals of data, taken at many different times, to estimate the scales of the waves. This makes it difficult to study the variability of ULF wave properties from one interval to another. It is therefore desirable to estimate the size of the ULF wave field at a particular time and location, both for understanding the details of wave-particle interactions, and for determining the coherency with which they drive the bow shock.

¹The Blackett Laboratory, Imperial College London, London, UK.

²Centre d’Etude Spatiale des Rayonnements, Centre National de la Recherche Scientifique, Toulouse, France.

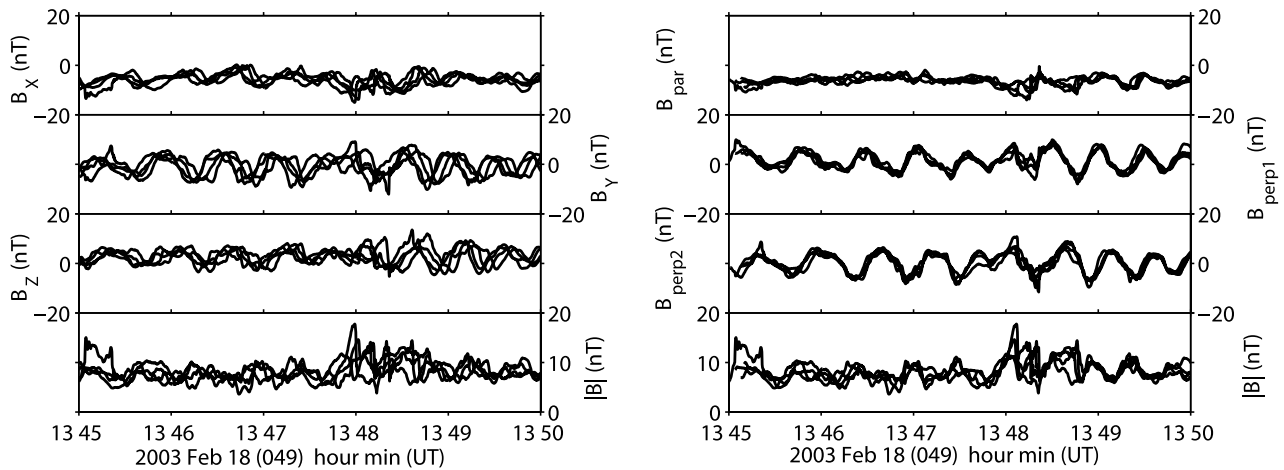


Figure 1. A 5-min interval of ULF waves. (left) Magnetic field time series measured by each of the four Cluster spacecraft in GSE coordinates. (right) Synchronized magnetic field time series rotated into a coordinate system where B_{par} is aligned to the wavevector, B_{perp1} is the component of the mean magnetic field perpendicular to the wavevector, and B_{perp2} completes the right-handed set.

[5] In this paper, a method is presented to determine the size and shape of ULF waves using only a short (~ 5 min) interval of data from several spacecraft. This method, which is similar to that proposed by Horbury [2000], combines data from pairs of spacecraft to calculate the wave frame autocorrelation function of the magnetic field and is discussed in the next section. This is followed by an analysis of an example interval, resulting in estimates of the size of the waves in various directions. Finally, results from several intervals are discussed, along with their consequences for phenomena in the foreshock.

2. Estimating the Spatial Correlation Function

[6] The data analyzed in this section was taken on 18 February 2003, when the four Cluster spacecraft were positioned in the foreshock at $(15.6, 0.5, -7.8) R_E$, in GSE coordinates, separated by ~ 6000 km. Figure 1 (left) shows the local magnetic field as measured by the onboard magnetometer on each of the four spacecraft [Balogh *et al.*, 2001], shown in GSE coordinates, for the interval 1345–1350 UT: Cluster observed large-amplitude ($|\delta\mathbf{B}|/B_0 \approx 1$), quasi-monochromatic ULF waves with a period of ~ 36 s during this time. During this interval the mean magnetic field was $(-5.9, 0.8, 2.6)$ nT and the solar wind speed, measured by the CIS instrument [Rème *et al.*, 2001], was $(-641, 22, 27)$ km/s.

[7] A single spacecraft time series, in the frame of the wave, is a spatial cut through the structure as the spacecraft moves through it. If the wave is traveling with a velocity \mathbf{v}_w with respect to the spacecraft, the measured time series $\mathbf{B}_{\text{obs}}(t)$ is given by

$$\mathbf{B}_{\text{obs}}(t) = \mathbf{B}(\mathbf{r}(t)) = \mathbf{B}(\mathbf{r}_0 - (t - t_0)\mathbf{v}_w), \quad (1)$$

where $\mathbf{B}(\mathbf{r})$ is the magnetic field in the frame of the wave and \mathbf{r}_0 is the position of the spacecraft at a time t_0 .

[8] To determine the size and shape of a ULF wave, it is useful to transform into its rest frame. In order to do this the velocity of the wave is required. Using the relative times at

which the four spacecraft observe a structure, it is possible to deduce its orientation and speed [e.g., Schwartz, 1998], assuming that the waves are planar and uniform over the scale of the spacecraft separations. Eastwood *et al.* [2002, 2003] used this procedure to determine the wave vector of ULF waves; the same method is used here. The relative timing differences between spacecraft were found from peaks of cross-correlations of a magnetic field component perpendicular to the mean magnetic field. From these a normal direction and corresponding speed along this normal were obtained. The normal (in GSE coordinates) was found to be $\mathbf{n} = (0.77, 0.13, -0.62)$, with an associated speed along it of $v_n = -497$ km/s. The normal was 15° from the mean magnetic field and 2° from the minimum variance direction: the minimum variance direction [Sonnerup and Cahill, 1967] is often used to identify the orientation of wave vectors. If the wave is planar, this normal is directed along the wave vector, and v_n is the speed of the wave relative to the spacecraft along it. Figure 1 (right) shows the magnetic field with the time series synchronized using the cross-correlation time lags, rotated into a right-handed, orthogonal coordinate system where B_{par} is in the direction of the normal, B_{perp2} is the cross-product of the normal and the mean magnetic field, and B_{perp1} is the cross-product of B_{perp2} and B_{par} . It can be seen that there is little variation of the field in the direction of the normal, consistent with the fluctuations being predominantly perpendicular to the wave vector. Hodograms (not shown) indicate that these waves are left-handed with respect to the magnetic field in the spacecraft frame.

[9] The velocity along the normal, v_n , is not, however, the total velocity of the wave with respect to the spacecraft because the solar wind convects the wave downstream. Taking this convection into account, the velocity of the wave relative to the spacecraft is given by

$$\mathbf{v}_w = \mathbf{v}_{\text{sw}} + (v_n - \mathbf{v}_{\text{sw}} \cdot \mathbf{n})\mathbf{n}, \quad (2)$$

where \mathbf{v}_{sw} is the solar wind velocity in the spacecraft frame. It was found that the velocity of the wave \mathbf{v}_w was $(-631,$

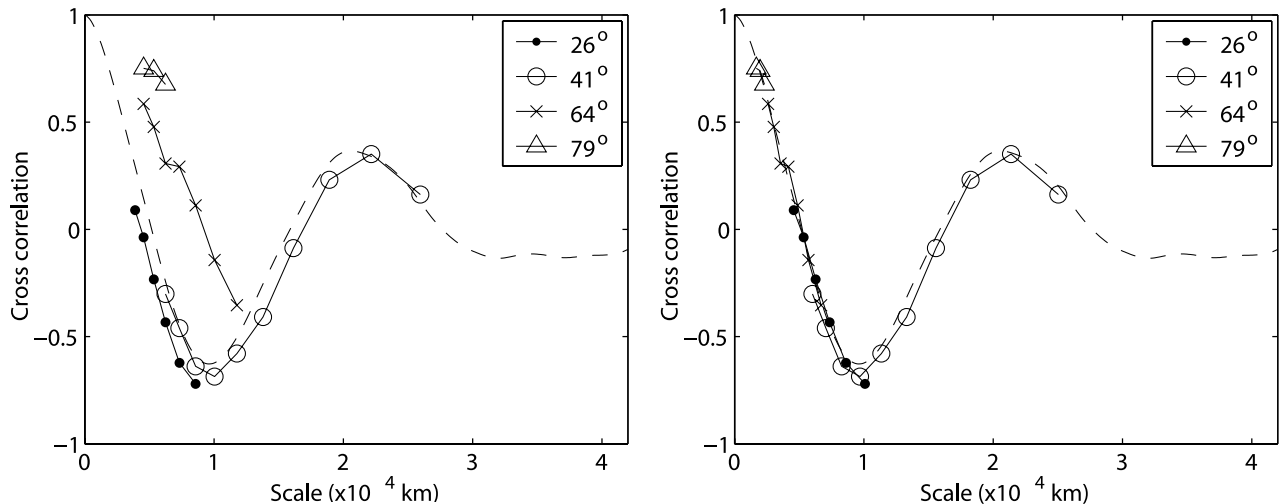


Figure 2. (left) Wave frame correlations of the magnetic field at various angles to the wavevector; dashed line is the wave frame single spacecraft autocorrelation (38° to wavevector) along the spacecraft velocity direction. (right) Wave frame correlations at the same angles but with scales multiplied by an angle-dependent factor to fit the single spacecraft autocorrelation.

24, 19) km/s in GSE coordinates and the speed of the wave in the solar wind frame was 13 km/s. This is rather low compared with the local Alfvén speed of around 70 km/s, which may reflect uncertainties in its determination resulting from relative timing uncertainties. However, since the solar wind velocity is much larger than the speed of ULF waves in the plasma frame, it is the orientation of the normal that is more important in this analysis.

[10] The autocorrelation of single spacecraft data as it travels through the wave gives a spatial sample of the variation of the wave in the direction of the spacecraft velocity ($-\mathbf{v}_w$). Since the ULF waves are quasi-monochromatic, the periodicity of the single spacecraft autocorrelation will be the same as that of the waves in this direction. Figure 2 (left) shows the wave frame single spacecraft autocorrelation (dashed line). The peak at $\sim 20,000$ km consequently gives the correlation length of the ULF waves in the direction of the spacecraft velocity. If the waves were infinite plane waves, the correlation length in the direction of the spacecraft velocity, which was 37° from the wave vector, would correspond to a wavelength of $20000 \cdot \cos(37^\circ)$ km, about $2.5 R_E$. This is comparable with previous estimates of ULF wavelengths [Hoppe and Russell, 1983; Le and Russell, 1990; Le et al., 1993].

[11] With a single spacecraft it is only possible to construct wave frame correlations in one direction. By cross-correlating the samples of two different spacecraft, however, variations of the magnetic field in the direction between the two sampling points can be measured. Hence to build up a picture of the shape of the wave in the wave frame, 5 vectors/s resolution magnetic field data from the interval shown in Figure 1 (right) were cross-correlated between all spacecraft pairs, using a component perpendicular to both the normal and the mean magnetic field (i.e., $B_{\text{perp}2}$). Different time lags from cross-correlating each pair of spacecraft correspond to varying the separation of the two sampling points, as viewed in the wave frame. Therefore the cross-correlations vary with time lag because they are essentially varying spatial correlations in the wave

frame. These separations in the wave frame can be found from the time lags through the following equation

$$\mathbf{s}_{ij}(t) = \mathbf{r}_{ij} - \mathbf{v}_w t, \quad (3)$$

where $\mathbf{s}_{ij}(t)$ is the separation vector in the wave frame for spacecraft i and j , \mathbf{r}_{ij} is the position of spacecraft i relative to j and t is the time lag in the cross-correlation. This leads to estimates of the wave frame spatial autocorrelation of the magnetic field at many scales and in many directions. The range of scales and directions obtained for the data interval in Figure 1 is shown in Figure 3.

[12] To order this information, the wave frame correlations were placed into bins, depending on the magnitude of the separation vector and its angle to the wave vector. The angular bins were 7.5° wide and there were 40 logarithmically spaced scale bins between 50 and 28,000 km, that is, at every scale there were 12 bins which between them covered angles between 0 and 90° . The edges of these bins are delineated in Figure 3 by dashed lines. The spatial autocorrelation in the wave frame for each bin in angle and scale was taken to be the average of all points in that bin.

[13] It is clear from Figure 3 that not all bins contained any data points and indeed most contained none: the number of points in each bin varied from 0 to ~ 100 . Bins containing fewer than two points were discarded. The number of points in each bin depends on the formation of the four spacecraft, the orientation of the wave and the velocity of the wave relative to the spacecraft. This binning procedure results in estimates of the wave frame magnetic field autocorrelation for a wide range of scales and angles.

[14] The wave frame correlations from a few selected angles from the wave vector, as well as the single spacecraft autocorrelation, are shown in Figure 2 (left). If the shape of the wave in all directions is approximately the same but with a different correlation length, one would expect the wave frame correlations at different angles from the wave vector to be the same shape (i.e., have the same functional form) as that of the single spacecraft autocorrelation but to

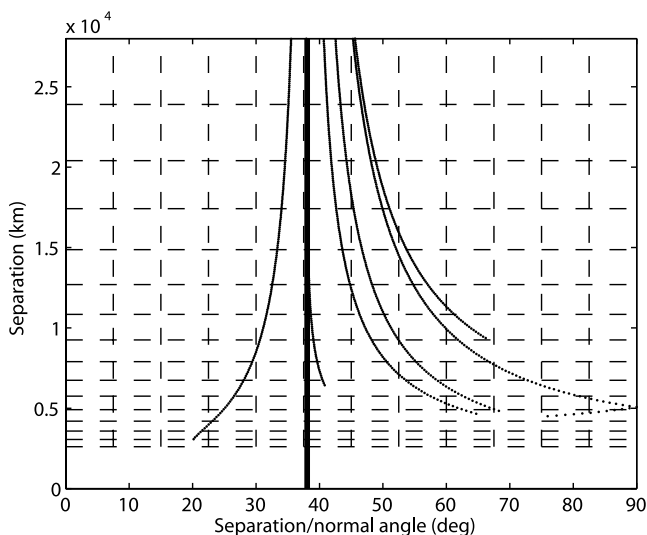


Figure 3. Wave frame separation scales and angles from the wavevector sampled by cross-correlating data from pairs of Cluster spacecraft for the ULF wave interval shown in Figure 1. Each curved line of dots results from correlations between one pair of spacecraft. The vertical solid line shows the angle sampled by a single spacecraft autocorrelation. Dashed vertical and horizontal lines delineate the ranges of angles and separations used to bin the data.

vary on a different spatial scale. Figure 2 (left) shows this to be the case: other angles, not shown in the figure, exhibit similar behavior. In Figure 2 (right) the wave frame correlations are shown with the spatial axis rescaled by a linear factor for each angle so that the data collapses onto the dashed line: this linear factor was calculated by minimizing the squared deviation of the data at each angle from the single spacecraft autocorrelation. This results in good agreement between the single spacecraft autocorrelation and the data from wave frame cross-correlations between spacecraft.

[15] From the calculated scale factors it is possible to deduce the correlation length of the wave at each particular angle, by dividing the absolute correlation length obtained from the single spacecraft autocorrelation by the corresponding scale factor for that angle. This procedure results in estimates of the correlation length of the ULF wave at a number of angles from the wave vector, as required. Estimates of this correlation length at different angles to the wave vector are shown in Figure 4 (top).

3. Size and Shape

[16] The correlation length of an infinite plane wave in different directions to its wave vector is given by

$$\lambda(\theta) = \frac{\lambda_0}{\cos(\theta)}, \quad (4)$$

where λ is the wavelength and θ is the angle from the wave vector. This infinite plane wave solution is depicted by the dashed line in Figure 4 (top), where the constant λ has been calculated from the single spacecraft autocorrelation value (the open circle). The infinite plane wave is a good fit to the

data for small values of θ . On the basis of this assumption, the correlation length along the wave vector (i.e., the wavelength) is $\sim 2.5 R_E$, consistent with previous estimates [Le and Russell, 1990; Le et al., 1993]. However, while the measured correlation length is large at large angles from the wave vector (dots in Figure 4 (top)), it is significantly lower than expected for an infinite plane wave. The correlation length perpendicular to the wave vector is around $10 R_E$. The ULF waves were therefore finite in extent perpendicular to the wave vector.

[17] Since the analysis in this paper assumes that the ULF waves were azimuthally symmetric about the wave vector, the full three-dimensional (3-D) representation of the size of the waves in all directions is a surface of revolution. Therefore one only need consider a cross section of the wave centered on the wave vector to represent its “shape,” that is, the amplitude of the correlation length in a variety of directions. This is diagrammatically shown in Figure 4 (bottom), where the wave vector lies along the y-axis.

[18] In order to parameterize the scale of the ULF wave parallel and perpendicular to the wave vector, the data was approximated as an oblate spheroid, through a least squares method. The elliptical cross section of the oblate spheroid is shown as the solid line in both parts of Figure 4. The fit

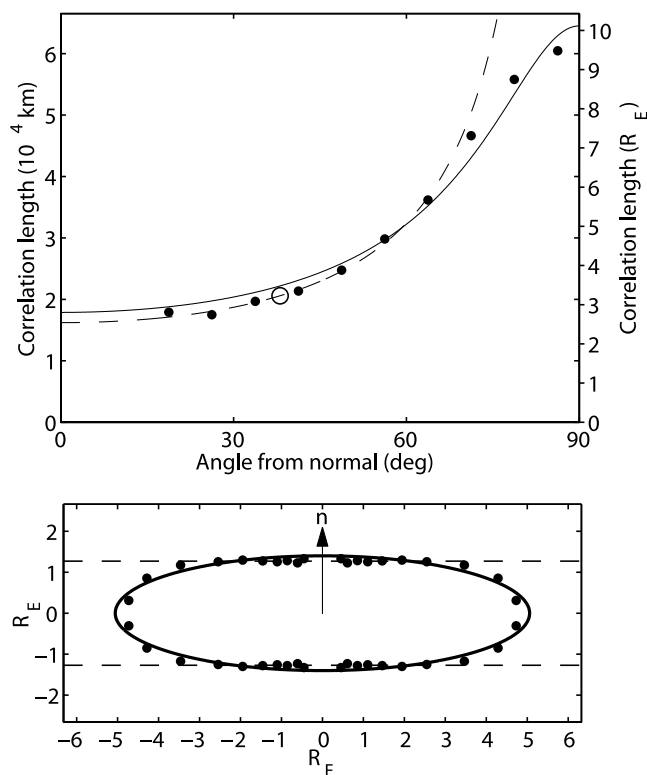


Figure 4. (top) Correlation length as a function of angle from the wave vector including infinite plane wave solution (dashed line) and fit to oblate spheroid (solid line). The single spacecraft autocorrelation point is shown as a circle. (bottom) Quantitative diagram of the “shape” of ULF waves, obtained by tracing out the correlation length of the waves in various directions. Infinite plane wave (dashed line) and oblate spheroid (solid line) fits are also shown. The wavevector points vertically (to the top of the page).

yields parallel (λ_{\parallel}) and perpendicular (λ_{\perp}) correlation lengths of 17,876 km (2.8 R_E) and 64,511 km (10.1 R_E), respectively, the ratio of these being 3.7.

[19] However, it is clear from Figure 4 that the ULF waves are not exactly described by an oblate spheroid: the correlation length is overestimated at both small and large angles from the wave vector and underestimated at intermediate angles. Indeed, at lower angles the correlation lengths much more closely resemble the plane wave solution than the oblate spheroid. This tendency toward planarity close to the wave vector extends over a distance of $\sim 20,000$ km ($\sim 3 R_E$), implying that ULF waves are coherent and have a planar wave front over such scales. This supports the assumptions made in determining the frame of the wave through multi-spacecraft analyses [Eastwood *et al.*, 2002; Eastwood *et al.*, 2003], which assumed the waves were uniform and planar over the separations of the spacecraft.

4. Discussion

[20] By estimating the spatial correlation function of ULF waves as a function of the angle between the separation vector and the wave vector in the wave frame, the size and shape of the waves have been determined. The overall shape of the waves can be approximated as an oblate spheroid, symmetric about the wave vector, but they were planar on scales of $\sim 3 R_E$ perpendicular to this direction. To establish the reliability of this result, the same analysis was performed on seven other intervals of ~ 30 s ULF waves, some of which contained additional fluctuations such as phase steepened waves and high-frequency whistlers. The results produced were similar to those already determined from the interval in Figure 1. The wavelength was typically 1–3 R_E and the correlation length perpendicular to the wave vector 8–18 R_E . The ratio $\lambda_{\perp}/\lambda_{\parallel}$ for the waves was generally between 3 and 8. The oblate spheroid proved to be a good approximation to the overall shape of the ULF waves but with more planar behavior close to the normal over scales of a few R_E .

[21] These consistent results over a number of intervals suggest that the method used here is reliable. We estimate the errors in derived quantities, such as the correlation lengths, to be ~ 10 –20%. One problem in using this method, however, is finding suitable data intervals. Because the method implicitly assumes statistical homogeneity, only intervals with approximately constant amplitude waves can be used. In order to identify the size of the waves in different directions, each spacecraft needs to see very similar phenomena (so that the wave vector can be identified using timing analysis), but there also need to be significant differences between each spacecraft: without such differences the method will produce an infinite plane wave solution when it extrapolates outside the separations of the spacecraft. This also occurs for intervals which are too short (~ 1 –2 min). The best interval length is typically 3–5 min, containing several full oscillations.

[22] One common problem in finding suitable intervals is angular coverage. This is a result of the formation and orientation of the spacecraft to the wave. Ideally, one would like reasonable coverage throughout all angular bins, but it is often the case that some bins do not contain many

correlation points whereas others contain many. This significantly limits the applicability of the method.

[23] Previous estimates of the scale sizes of ULF waves by [Le and Russell, 1990; Le *et al.*, 1993] examined correlation coefficients as a function of the separation of the two ISEE spacecraft transverse to the solar wind velocity and found the coherence length (defined to be the point where the correlation coefficient drops to 0.5) perpendicular to the solar wind velocity to be $\sim 1 R_E$. From Figure 2 it can be seen that for this example interval, the scale point of 0.5 on the dashed line corresponds to a separation along the spacecraft velocity of ~ 3000 km, which is about 7 times smaller than the correlation length in the direction of the flow. The angle between the wave vector and the solar wind velocity vector was 37° ; hence the angle between the direction perpendicular to the solar wind velocity and the wave vector was 53° . From Figure 4 (top) this leads to a coherence length perpendicular to the flow of ~ 4000 km or $\sim 0.7 R_E$, consistent with that of [Le and Russell, 1990; Le *et al.*, 1993] and other estimates using different techniques [e.g., Eiges *et al.*, 2001]. However, the method presented here makes it possible simultaneously to measure the size of the waves in different directions from only a few wave periods.

[24] The large-amplitude changes in magnetic field direction due to ULF waves result in quasi-periodic changes in θ_{Bn} , and hence the shock characteristics [Greenstadt and Mellott, 1985] and backstreaming ions [Meziane *et al.*, 2004b]. The relatively large extent of the ULF waves perpendicular to their normal (8–18 R_E) therefore implies that changes in the upstream magnetic field at the shock surface are coherent over a similarly large area of the shock. Owing to the relative orientation of the ULF waves and the shock surface, one would expect a spatial modulation in the magnetic field at the shock with a periodicity of, typically, a few R_E .

[25] The question arises as to the physical origin of the scale of the waves perpendicular to their wave vector. The scale is much bigger than a reflected ion gyroradius. Indeed, the extent of the waves (8–18 R_E) is comparable to the typical size of the quasi-perpendicular region of the bow shock and may therefore be the result of a coherent generation of ULF waves over the entire quasi-perpendicular foreshock. Further analysis, with larger separations between spacecraft, would be required in order to test this hypothesis.

[26] Since the ULF waves are of finite size, one would expect that there should be some clear evidence of this within the data as observed by the spacecraft. The time taken for the spacecraft to cross the correlation length along the wave vector, that is, the wavelength, results in the familiar ~ 30 s periodicity that is observed, given by

$$t_{\parallel} = \frac{\lambda_{\parallel}}{|\mathbf{v}_w \cdot \mathbf{n}|}. \quad (5)$$

However, the time for the spacecraft to traverse the larger perpendicular scale is given by

$$t_{\perp} = \frac{\lambda_{\perp}}{|\mathbf{v}_w - (\mathbf{v}_w \cdot \mathbf{n})\mathbf{n}|} \quad (6)$$

and is typically a few minutes. One might expect to see evidence of this timescale in the data, perhaps as a

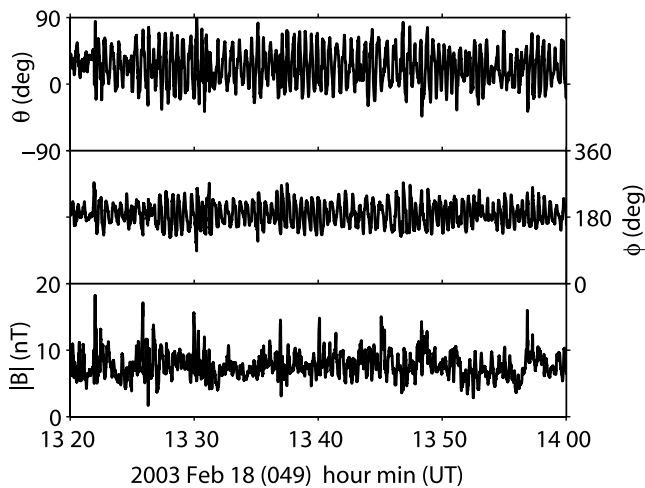


Figure 5. An extended interval of ULF waves 1320–1400 UT. The quasi-periodic enhancements in the field magnitude and modulation of the field amplitude might result from the spacecraft traversing the perpendicular scale of the ULF waves.

modulation of the wave amplitudes. To investigate any consequences of this time scale the extended interval 1320–1350 UT, as shown in Figure 5, was considered and split into 10 consecutive subintervals of 3 min. Six of these intervals resulted in reliable estimates of the size, shape, and orientation of the ULF waves, with typical wave vector-parallel scales (wavelengths) of $\sim 16,000$ km and $\lambda_{\perp}/\lambda_{\parallel}$ ratios of ~ 6 . Estimates of the time taken to traverse the perpendicular scale ranged from 2 to 5 min. A series of enhancements in the magnetic field magnitude is visible in Figure 5, typically separated by a few minutes, reminiscent of SLAMS seen at quasi-parallel shocks [e.g., Lucek et al., 2004]. These enhancements are accompanied by high-frequency whistler waves (not visible in Figure 5) that are not observed elsewhere in the interval. There also appears to be a small variation in the amplitude of the ULF waves with around the same period. This may be the result of the spacecraft traversing the perpendicular extent of the waves. One would not expect to see field enhancements at the edges of ULF waves, but this may be due to the unusual orientation of the background magnetic field during this time: the average field was only 21° from the local bow shock normal (on the basis of the Peredo et al. [1995] model). Therefore without the presence of the ULF waves, the shock would have been quasi-parallel. At the edges of ULF wave packets, where the wave amplitude would be expected to be small, the shock could therefore have been nearly parallel, resulting in many more backstreaming particles from the shock and the generation of nonlinear SLAMS-like structures. This may therefore explain the semiperiodic magnetic field enhancements visible in Figure 5. However, one would not expect to observe such enhancements during all ULF wave intervals. Indeed, an examination of several other extended intervals of ULF waves did not reveal such clear variations. Nevertheless, some variability on timescales similar to the predicted traversal times of the perpendicular scale, which can typically vary from 2 to 10 min, can sometimes be seen,

and ULF wave amplitudes are often modulated over such scales. These results suggest that the finite perpendicular extent of ULF waves may result in a modulation of their properties, on scales of a few minutes, in spacecraft data.

[27] Kis et al. [2004] have recently studied Cluster measurements of the diffuse ion population upstream of the bow shock during an extended interval, which includes the period shown in Figure 5, and derived their spatial density gradients. A future comparison of these energetic ion gradients with the wave characteristics deduced in this paper may help to constrain theories of wave-particle scattering and diffusive particle acceleration.

[28] This paper has presented the first results of a method to determine the size and shape of ULF waves. Future work will address the relation of these parameters to ion distributions in the foreshock, for example, how the correlation lengths are related to the backstreaming ions, and their consequences for the modulation of the shock itself. It may also be possible to extend this method to estimate the full 3-D shape of the waves and therefore study their refraction and steepening.

[29] **Acknowledgments.** Cluster work at Imperial College London is funded by PPARC (UK); T. Horbury is supported by a PPARC Fellowship.

[30] Lou-Chuang Lee thanks the two reviewers for their assistance in evaluating this paper.

References

- Balogh, A., et al. (2001), The Cluster magnetic field investigation: Overview of inflight performance and initial results, *Ann. Geophys.*, *19*, 1207–1217.
- Burgess, D. (1997), What do we really know about upstream waves?, *Adv. Space Res.*, *20*, 673–682.
- Eastwood, J. P., A. Balogh, M. W. Dunlop, and T. S. Horbury (2002), Cluster observations of fast magnetosonic waves in the terrestrial foreshock, *Geophys. Res. Lett.*, *29*(22), 2046, doi:10.1029/2002GL015582.
- Eastwood, J. P., A. Balogh, E. A. Lucek, C. Mazelle, and I. Dandouras (2003), On the existence of Alfvén waves in the terrestrial foreshock, *Ann. Geophys.*, *21*, 1457–1465.
- Eiges, P. E., G. N. Zastenker, J. Safrankova, Z. Nemecek, and N. A. Eismont (2001), Statistical approach to the evaluation of the mean correlation length and the propagation velocity of middle-scale plasma structures in the Earth's foreshock, *Cos. Res.*, *39*, 432–438.
- Gary, S. G. (1985), Electromagnetic ion beam instabilities: Hot beams at interplanetary shocks, *Astrophys. J.*, *88*, 342–352.
- Greenstadt, E. W., and M. M. Mellott (1985), Variable field-to-normal shock-foreshock boundary observed by ISEE-1 and -2, *Geophys. Res. Lett.*, *12*, 129–132.
- Hoppe, M. M., and C. T. Russell (1983), Plasma rest frame frequencies and polarizations of low-frequency upstream waves: ISEE 1 and 2 observations, *J. Geophys. Res.*, *88*, 2021–2028.
- Horbury, T. S. (2000), Cluster II analysis of turbulence using correlation functions, in *Proceedings of Cluster II Workshop on Multiscale/Multi-point Plasma Measurements, SP-449*, edited by R. A. Harris, pp. 89–97, ESA Publ. Div., Noordwijk, Netherlands.
- Kis, A., M. Scholer, B. Klecker, E. Möbius, E. A. Lucek, H. Rème, J. M. Bosqued, L. M. Kistler, and H. Kucharek (2004), Multi-spacecraft observations of diffuse ions upstream of Earth's bow shock, *Geophys. Res. Lett.*, *31*, L20801, doi:10.1029/2004GL020759.
- Le, G., and C. T. Russell (1990), A study of the coherence length of ULF waves in the Earth's foreshock, *J. Geophys. Res.*, *95*, 10,703–10,706.
- Le, G., C. T. Russell, and D. S. Orłowski (1993), Coherence lengths of upstream ULF waves: Dual ISEE observations, *Geophys. Res. Lett.*, *20*, 1755–1758.
- Lucek, E., T. Horbury, A. Balogh, I. Dandouras, and H. Rème (2004), Cluster observations of structures at quasi-parallel bow shocks, *Ann. Geophys.*, *22*, 2309–2313.
- Mazelle, C., et al. (2003), Production of gyrating ions from nonlinear wave-particle interaction upstream from the Earth's bow shock: A case study from Cluster-CIS, *Planet. Space Sci.*, *51*, 785–795.
- Meziane, K., C. Mazelle, R. P. Lin, D. LeQuéau, D. E. Larson, G. K. Parks, and R. P. Lepping (2001), Three-dimensional observations of gyrating ion distributions far upstream from the Earth's bow shock and their

- association with low-frequency waves, *J. Geophys. Res.*, *106*, 5731–5742.
- Meziane, K., et al. (2004a), Simultaneous observations of field-aligned beams and gyrating ions in the terrestrial foreshock, *J. Geophys. Res.*, *109*, A05107, doi:10.1029/2003JA010374.
- Meziane, K., et al. (2004b), Bow shock specularly reflected ions in the presence of low-frequency electromagnetic waves: A case study, *Ann. Geophys.*, *22*, 2325–2335.
- Peredo, M., J. A. Slavin, E. Mazur, and S. A. Curtis (1995), Three-dimensional position and shape of the bow shock and their variation with Alfvénic, sonic and magnetosonic Mach numbers and interplanetary field orientation, *J. Geophys. Res.*, *100*, 7907–7916.
- Rème, H., et al. (2001), First multispacecraft ion measurements in and near the Earth's magnetosphere with identical cluster ion spectrometry (cis) experiment, *Ann. Geophys.*, *19*, 1303–1354.
- Schwartz, S. J. (1998), Shock and discontinuity normals, mach numbers, and related parameters, in *Analysis Methods for Multi-Spacecraft Data*, edited by G. Paschmann and P. Daly, pp. 249–270, ESA Publ. Div., Noordwijk, Netherlands.
- Sonnerup, B. U. Ö, and L. J. Cahill (1967), Magnetopause structure and attitude from Explorer 12 observations, *J. Geophys. Res.*, *72*, 171–183.
-
- M. Archer, A. Balogh, T. S. Horbury, and E. A. Lucek, The Blackett Laboratory, Imperial College London, Prince Consort Road, London SW7 2BW, UK. (t.horbury@imperial.ac.uk)
- I. Dandouras and C. Mazelle, Centre d'Etude Spatiale des Rayonnements, Centre National de la Recherche Scientifique, 9 Avenue du Colonel Roche, F-31028 Toulouse, France.